Nigerian Journal of Technology (NIJOTECH)
Vol. 44, No. 3, September, 2025, pp.411 - 421
www.nijotech.com

Print ISSN: 0331-8443
Electronic ISSN: 2467-8821
https://doi.org/10.4314/njt.v44i3.5

SYNERGISTIC MANGANESE OXIDE AND COCONUT HUSK NANOPARTICLES HYBRID COATING FOR SUSTAINABLE PIPELINE CORROSION CONTROL IN ACIDIC ENVIRONMENT

AUTHORS:
P. A. Oghenekowho[1*], C.I. Ajuwa[1], B.U. Oreko[1]

AFFILIATIONS:
[1] Department of Mechanical Engineering, Federal University of Petroleum Resources Effurun, Delta State

***CORRESPONDING AUTHOR:**
Email: oghenekowho.aruoture@fupre.edu.ng

ARTICLE HISTORY:
Received: November 09, 2024
Revised: June 23, 2025
Accepted: September 07, 2025
Published: October 15, 2025.

KEYWORDS: Corrosion, Novel Hybrid coating, Epoxy resin, Nanoparticles, Petroleum pipelines, EIS, PDP

ARTICLE INCLUDES:
Peer review

DATA AVAILABILITY:
On request from author(s)

EDITORS:
Chidozie Nnaji

FUNDING:
None

Abstract

In the oil and gas industry, corrosion is a major problem that can result in pipeline breakdowns and economic losses. This project aims to develop a novel hybrid corrosion protection coating for petroleum pipeline-grade steel using epoxy resin reinforced with manganese oxide and coconut husk nanoparticles (CHNP). Response Surface Methodology was used to develop and optimise the hybrid coating (RSM). Potentiodynamic polarisation (PDP) and Electrochemical Impedance Spectroscopy (EIS) techniques were used to assess its performance. The findings showed that the corrosion resistance of the developed hybrid coating was greatly enhanced by the addition of CHNP and MNO_2, *and a maximum corrosion efficiency of 93% was attained at 4.45 weight percent CHNP and 2.03 weight percent* MNO_2 *in 0.5* $mol.dm^{-3}$ H_2SO_4. *The results obtained showed that the combination of CHNP and* MnO_2 *is suitable for formulating corrosion protection coating for carbon steels.*

1.0 INTRODUCTION

Carbon steels have proven to be highly effective in the transportation of petroleum products for numerous years [1]. This is due to their exceptional tensile strength and fracture toughness [2]. Nevertheless, despite their excellent mechanical properties, carbon steels are prone to corrosion, which can lead to premature failure. This failure typically results in a waste of time, resources, and harm to the environment [3, 4]. Corrosion poses a serious threat to the global manufacturing industry, with estimated annual losses, according to the World Corrosion Organisation, amounting to US$2.5 trillion worldwide [5]. Nigeria, according to the Nigeria Extractive Industries Transparency Initiative (NEITI), lost 270 million barrels of crude oil estimated at $14.6 billion between 2016 and 2020 as a result of corrosion and other factors [6].

These losses are massive and have caught the attention of researchers who are focused on finding solutions. One area that is enjoying attention is the

HOW TO CITE:
Oghenekowho, P.A, Ajuwa, C.I., and Oreko, B. U. "Synergistic Manganese Oxide and Coconut Husk Nanoparticles Hybrid Coating for Sustainable Pipeline Corrosion Control in Acidic Environment.", *Nigerian Journal of Technology*, 2025; 44(3), pp. 411 – 421; https://doi.org/10.4314/njt.v44i3.5

development of advanced coatings that can effectively protect carbon steels from corrosion, even in the most challenging environments [7, 8, 9].
Various types of corrosion coatings, such as inorganic coatings [10], organic coatings [11, 12, 13], hybrid coatings [14], eco-friendly coatings [15, 16] and self-healing coatings [17, 18] have been created to address the issue of corrosion in carbon steels.

However, in recent years, nanotechnology has become a promising avenue for corrosion protection, providing customised solutions that integrate advanced materials with sustainability [19]. Nanoparticles of oxides of metals like aluminium, titanium, zinc, and cobalt [20, 21, 22, 23] have been used to develop protective coatings for carbon steels. Also, nanoparticles from agro-wastes like egg shells, oil palm fronds, palm kernel shells, cashew nut shells, walnut husks and coconut husks [24, 25, 26] have been used successfully in combination with other materials to develop corrosion-protective coatings for carbon steels. Despite the growing interest in nature-based nanoparticles as a solution to corrosion problems, no report of the use of coconut husk in combination with manganese oxide for the production of corrosion protective coating for carbon steels has been documented.

This study focuses on developing an eco-friendly hybrid coconut husk/manganese oxide corrosion protection coating for pipeline-grade carbon steels. More specifically, the research will examine the combined effects of manganese oxide and coconut husk nanoparticles in this coating. By harnessing the unique properties of both materials, this study aims to develop an efficient and eco-friendly coating (eco-shield) capable of withstanding aggressive environmental conditions obtainable in the oil and gas sector.

Upon completion, this work will provide a sustainable and cost-effective solution for corrosion mitigation, while making a significant contribution to the growing research domain of green nanocomposite corrosion coatings for protecting critical infrastructure.

2.0 METHODOLOGY

2.1 Design of Experiment

RSM central composite design was applied to design the experiment. The designed experiment using RSM is shown in Table 1. The factors considered for the design were acid concentration in mol/dm^3, coconut husk nanoparticles in weight percent, and manganese oxide in weight percent.

Table 1: The Detailed Design of the Experimental Variables

Run	H_2SO_4 (mol/dm^3)	CHNP (%. wt.)	MnO_2 (%wt.)
1	1	1.81	1.81
2	2	1.81	1.81
3	1	4.18	1.81
4	2	4.18	1.81
5	1	1.81	4.18
6	2	1.81	4.18
7	1	4.18	4.18
8	2	4.18	4.18
9	0.5	3	3
10	2.5	3	3
11	1.5	1	3
12	1.5	5	3
13	1.5	3	1
14	1.5	3	5
15	1.5	3	3
16	1.5	3	3
17	1.5	3	3
18	1.5	3	3
19	1.5	3	3
20	1.5	3	3

2.2 Sample Preparation

The specimens for the various tests were cut from a cylindrical carbon steel crude oil pipeline. The chemical composition of the carbon steel is given in Table 2. Each specimen is machined to a dimension of 4cm × 4cm × 0.5cm. The surfaces of the specimens underwent successive polishing using 60, 80, 250, 400 and 600 grit SIC paper in line with [27], followed by rinsing with distilled water and degreasing with acetone. To facilitate easy suspension during coating, drying, and distinct identification during corrosion testing, a 5mm diameter hole was drilled on the upper centre edge of each metal specimen. A thread was then attached through the hole to allow the specimen to be hung securely

https://doi.org/10.4314/njt.v44i3.5

Table 2: Elemental composition of carbon steel specimen

Element	Fe	C	Mn	S	Cu	Si	P	Ca	Ti	V	Cr	Ni	Al	Mo
Comp. (%wt.)	balance	0.67	0.58	0.01	0.21	0.06	0.01	0.1	0.01	0.02	0.04	0.02	0.04	0.21

2.3 Coconut Husk Nanoparticles (CHNP) Synthesis

A mechanical milling device (PM100 series) was used to create the coconut husk nanoparticles. The fibrous husks of the coconut were physically removed from the endocarp, cleaned to get rid of any dirt or foreign objects, and then left to dry for three days in the sun. Figure 1 illustrates the sequence of steps used to crush the dried husks, and a magnetic sieve of 75µm was used to sieve it. After that, the synthesized CHNP was characterized and kept in an airtight container.

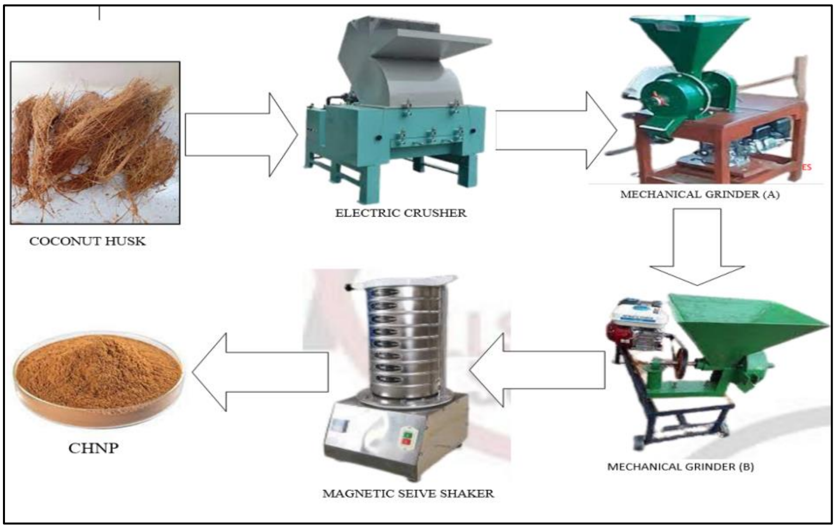

Figure 1: Coconut husk nano-sizing process

The chemical composition of the synthesized CHNP is given in Table 3

Table 3: Chemical composition of CHNP

S/N	COMPONENT	COMPOSITION (%)
1	Cellulose	26
2	Hemicellulose	18
3	Lignin	42
4	Others	14

2.4 Coating Preparation

After preparing the epoxy matrix (epoxy resin/hardener in a 2:1 ratio) it was thoroughly mixed to obtain a uniform consistency. The appropriate amounts of the epoxy matrix, CHNP, and MNO_2 (with an average size of 65-100nm [28] and percentage purity of 99.4%) were measured using an electric-sensitive weighing machine following the design table. To avoid localised concentrations of nanoparticles and preserve their uniform dispersion within the epoxy resin matrix, the mixture of CHNP and MNO_2 was introduced gradually to the epoxy matrix. The mixture was agitated for a further half hour at 500 revolutions per minute with an electrically powered anchor stirrer.

2.5 Coating Application and Curing

Twenty carbon steel specimens in all were ready for coating. As soon as the coating preparation was complete, each specimen was dipped once into the custom-made coating mixture to guarantee complete coverage and consistent coating thickness. To accomplish thorough curing and hardening of the epoxy resin matrix, each specimen was carefully dipped into the correct coating mixture and allowed to drain any excess of the coating mixture before being suspended in direct sunshine for three (3) days. All specimens were assumed to have the same coating thickness since they were dipped in a homogeneous mixture for the same period. The adhesion strength of the coating was determined using the cross-cut tape test, as per the ASTM D3359 standard.

2.6 Electrochemical Corrosion Measurement

A Model 600E Series Electrochemical Analyzer/Workstation was used for the

https://doi.org/10.4314/njt.v44i3.5

electrochemical studies. A three-electrode cell with 250 ml of test fluid was used to carry out the experiments. The reference electrode (RE) was a silver chloride electrode (Ag/AgCl), the counter electrode was a platinum mesh, and the working electrode (WE) was an epoxy-resin mounted sample with an exposed surface area of 16 cm^2.

2.6.1 Open Circuit Potential (OCP)

To guarantee that the corrosion potential is reliably recorded, the open-circuit potential (OCP) test was performed to determine the specimen's (working electrode) potential without interfering with the electrochemical reactions on its surface.

2.6.2 Potentiodynamic Polarization (PDP)

The coated carbon steel electrode was submerged in the test solution for 300 seconds at the open circuit potential (E_{ocp}) to get the system into a steady condition before each measurement. The coated specimen was submerged in diluted H_2SO_4 before carrying out the potentiodynamic polarisation test. The potential was passed from -1.5 to +1.5 V at a scan rate of 0.01Vs^{-1}. The potential (E) and current density (i) were recorded during the entire scan. The results were analysed at the E_{ocp}. The Tafel plots generated from the electrochemical investigation were extrapolated to get the corrosion parameters, which included the cathodic, polarisation resistance (R_P), anodic Tafel slopes (β_a and β_c), and corrosion potential (E_{corr}) and current density (i_{corr}). Equation 1 was used to assess the protective effectiveness of the epoxy-reinforced coatings.

$$P.E = \frac{i_{corr\ uncoated} - i_{corr\ coated}}{i_{corr\ uncoated}} \times \frac{100}{1} \quad (1)$$

Where P.E = protective efficiency (%) calculated using i_{corr} values

2.6.3 Electrochemical Impedance Spectroscopy (EIS)

A small sinusoidal AC (alternating current) voltage signal was applied to the working electrode to start the EIS test at the E_{ocp} (the potential of an electrode when no current is flowing). The initial potential (Init E), high frequency (High Freq), and low frequency (Low Freq) were set to 1 V, 100kHz, and 1 Hz, respectively. This signifies that the EIS parameters were measured with an amplitude of 0.005V around OCP for frequency response, starting from high frequency 100000 Hz to low frequency 1 Hz. An approach known as Fourier transform (Imp FT) was used to gather the impedance data. At each frequency point, the impedance data, comprising the real (Z') and imaginary (Z") parts of the impedance, were recorded. The impedance parameters, including the solution resistance (R), double layer capacitance (C_{dl}), Cole-Cole resistance parameter, as well as charge transfer resistance (R_{ct}), were extracted by fitting the obtained impedance data (the Nyquist and Bode plots) to the appropriate equivalent circuit model portrayed in Figure 2. The impedance data is displayed in the Bode and Nyquist charts, respectively. Equation 2 was utilised to extrapolate the corrosion protection efficiency from R_{ct}. The extracted impedance parameters were employed to evaluate the epoxy-reinforced coatings' corrosion behaviour.

$$P.E = \frac{R_{ct\ coated} - R_{ct\ uncoated}}{R_{ct\ coated}} X \frac{100}{1} \quad (2)$$

Where P.E = protective efficiency (%) calculated using R_{ct} values

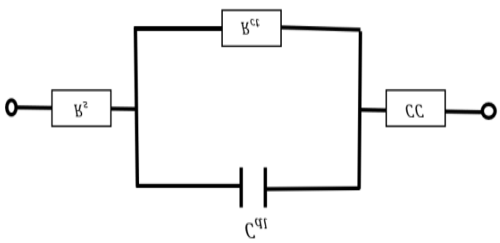

Figure 2: The Equivalent circuit model used to fit the impedance spectra of carbon steel

Where R_s is solution resistance of metal dissolution
R_{ct} is charge transfer resistance
C_{dl} is the double-layer capacitor
CC is the Cole-Cole resistance.

3.0 RESULTS AND DISCUSSION

3.1 Adhesion Strength

The adhesion strength test for the coating was found to be grade 3B, representing "moderate paint detachment, some squares removed at intersections and edges" using the ASTM D3359 standard for adhesion test grade classification. The photograph for the sample is shown in plate 1. This result shows that the developed coating has good adhesion strength, and this implies better adherence and a longer-lasting barrier against corrosion agents. The good adhesion strength could be due to the presence of a metallic oxide in the coating, as reported by [29].

3.1 PDP and OCP Result and Analysis

Values of all the electrochemical parameters, like corrosion potential (OCP) or E_{corr}, corrosion current

https://doi.org/10.4314/njt.v44i3.5

density (I_{corr}), corrosion rate, anodic Tafel slopes, and the cathodic Tafel slopes (β_a & β_c) obtained from potentiodynamic polarization (PDP) by Tafel extrapolation are presented in Table 4.

The corrosion rates of steel were calculated using Equation 3.

$$CR = \frac{87600 \times E_W \times I_{corr}}{n \rho F} \quad (3)$$

where I_{corr} is the corrosion density obtained by polarization curves, CR is the corrosion rates of steel (mm/year), E_W is the formula weight of carbon steel specimen (55.15 g/mol), ρ is the density of steel (7.85 g/cm^3), n is the chemical valence of ferric ion and F is the Faraday constant.

Plate 1: Photograph of the adhesion test tape of the sample

Table 4: Electrochemical parameters

Run/Sample	$E_{corr}(V)$	β_c (V/dec)	β_a(V/dec)	I_{corr} (A/cm^2)	Corrosion rate (mm/yr.)
1	-0.82	4.724	5.128	0.02459	20.908
2	-0.84	4.728	5.241	0.02557	21.364
3	-0.82	5.125	5.039	0.01442	12.234
4	-0.85	4.961	5.548	0.01980	16.689
5	-0.81	4.848	4.858	0.04634	39.860
6	-0.83	4.951	4.951	0.04880	40.316
7	-0.83	4.794	5.128	0.02309	20.186
8	-0.85	4.891	5.181	0.02391	20.640
9	-0.80	4.701	5.217	0.02361	20.392
10	-0.85	4.791	5.092	0.02503	21.158
11	-0.85	4.845	4.921	0.04511	37.320
12	-0.83	4.933	5.041	0.01722	14.230
13	-0.82	4.961	5.139	0.01761	14.838
14	-0.83	4.951	5.404	0.04323	36.712
15	-0.81	4.849	5.214	0.02491	21.075
16	-0.82	4.716	5.345	0.02244	18.875
17	-0.81	4.746	5.414	0.02332	19.793
18	-0.80	4.801	5.241	0.02353	19.775
19	-0.82	5.012	4.872	0.02212	18.812
20	-0.80	4.921	4.894	0.02422	20.775

https://doi.org/10.4314/njt.v44i3.5

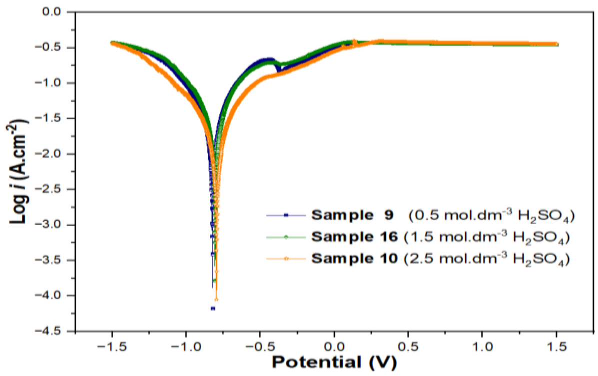

Figure 3: Polarization curves of carbon steel samples in (1.0, 2.0 and 2.5) M of H_2SO_4

The obtained corrosion potential (E_{corr}) for the designed coatings ranged from -0.85 to -0.80 V. A negative shift in corrosion potential was observed as the acid (H_2SO_4) concentration (in mol/dm^3) of the electrolyte solution increased. This can be viewed in the Tafel extrapolation plot of the experiment/run (9, 10 and 16) depicted in Figure 3. This implies that corrosion increases with an increment in the acidic concentration of the environment.

A positive shift in corrosion potential was observed as the coconut husk nanoparticle (CHNPs) content increased relative to the MnO_2 composition, as shown in Figures 4A and 4B. This positive shift indicates a better coating performance as it relates to corrosion resistance. The shift of E_{corr} towards positive value and a decrease in the I_{corr} value suggests the superior corrosion protection performance of the coatings whose composition of CHNPs is higher than the MnO_2 content.

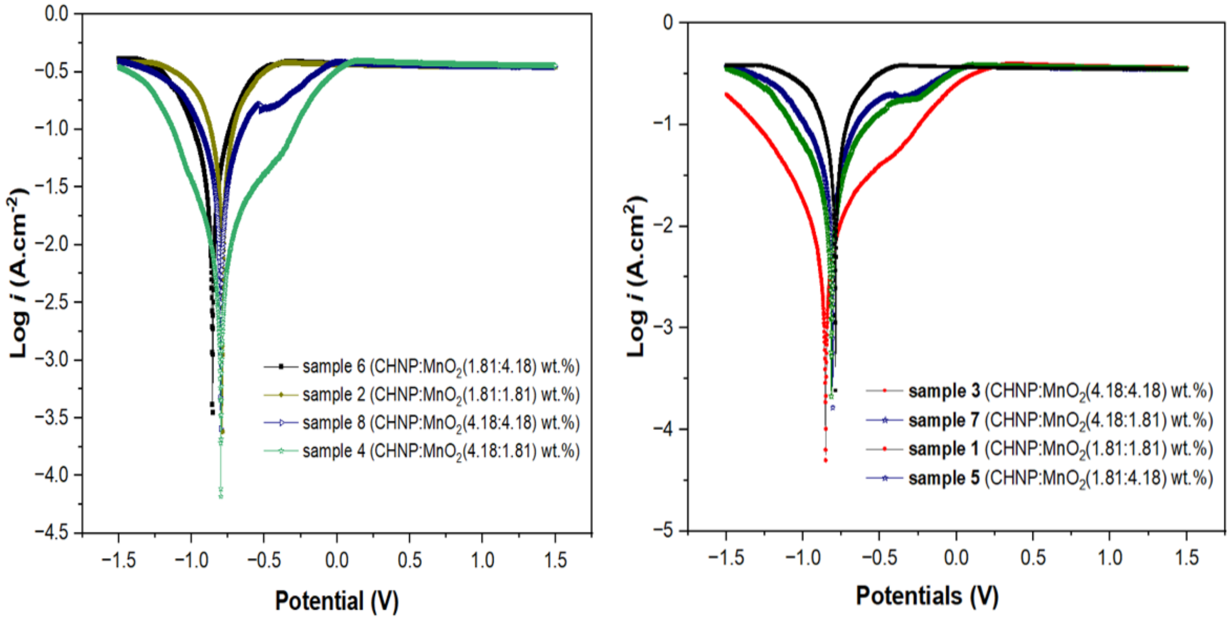

(A) (B)

Figure 4: Polarization curves of carbon steel **(A)** samples in 2.0 M H_2SO_4 and (**B**) samples in 1.0M of H_2SO_4 solution.

3.2 Response Surface Methodology

The calculated corrosion rate values placed alongside the RSM design are presented in Table 5.

The lowest corrosion rate of 12.23 mm/year was obtained with a CHNP and MnO_2 percentage composition of (4.18:1.81) wt. % and immersed in 1.0 M of H_2SO_4. The highest corrosion rate of 40.316 mm/year was reached when the acid concentration was 2.0 M and the CHNP composition was less than MnO_2. The observed results trend suggests that the corrosion protection that the designed coatings supplied was more effective when the acidic concentration (in mol/dm^3) of the corrosive medium and the MnO_2 content of the coatings were at the lowest level.

The ANOVA table for the RSM is given in Table 6. The p-value of the model, linear and square terms ($p<0.05$), showed that they are significant, but interactions involving acid concentrations were insignificant. This implies that although acid concentration affects the corrosion rate of the coating, its interaction with the other factors does not. The high R^2 value of the model, as shown in Table 7, shows that the model was able to explain the variability in the data.

https://doi.org/10.4314/njt.v44i3.5

Table 5: RSM design with three process parameters and response (corrosion rate) on carbon steel.

Run	Acid (Mol-dm^{-3})	CHNP (%. wt.)	MnO_2 (%wt.)	Corrosion rate (mm/yr)
1	1.00	1.81	1.81	20.908
2	2.00	1.81	1.81	21.364
3	1.00	4.18	1.81	12.234
4	2.00	4.18	1.81	16.689
5	1.00	1.81	4.18	39.860
6	2.00	1.81	4.18	40.316
7	1.00	4.18	4.18	20.186
8	2.00	4.18	4.18	20.640
9	0.50	3.00	3.00	20.392
10	2.50	3.00	3.00	21.158
11	1.50	1.00	3.00	37.320
12	1.50	5.00	3.00	14.230
13	1.50	3.00	1.00	14.838
14	1.50	3.00	5.00	36.712
15	1.50	3.00	3.00	21.075
16	1.50	3.00	3.00	18.875
17	1.50	3.00	3.00	19.793
18	1.50	3.00	3.00	19.775
19	1.50	3.00	3.00	18.812
20	1.50	3.00	3.00	20.775

Table 6: ANOVA Table showing the significance of the sources based on the p-value

Source	DF	Adj SS	Adj MS	F-Value	P-Value	Significance
Model	9	1362.12	151.347	185.88	0.000	Significant
Linear	3	1165.96	388.652	477.33	0.000	Significant
ACID CONC.	1	3.38	3.379	4.15	0.069	Significant
CHNP	1	613.07	613.073	752.95	0.000	Significant
MNO2	1	549.48	549.484	674.85	0.000	Significant
Square	3	107.59	35.863	44.04	0.000	Significant
ACID CONC.*ACID CONC.	1	1.12	1.123	1.38	0.267	Insignificant
CHNP*CHNP	1	59.24	59.239	72.75	0.000	Significant
MNO2*MNO2	1	59.29	59.29	72.82	0.000	Significant
2-Way Interaction	3	88.51	29.502	36.23	0.000	Significant
ACID CONC.*CHNP	1	1.99	1.988	2.44	0.149	Insignificant
ACID CONC.*MNO2	1	2.01	2.01	2.47	0.147	Insignificant
CHNP*MNO2	1	84.51	84.508	103.79	0.000	Significant
Error	10	8.14	0.814			
Lack-of-Fit	5	3.75	0.75	0.85	0.567	Insignificant
Pure Error	5	4.39	0.879			
Total	19	1370.26				

https://doi.org/10.4314/njt.v44i3.5

Table 7: Model Summary

Standard Deviation of Residuals	R-sq	R-sq(adj)	R-sq(pred)
0.902345	99.41%	98.87%	97.22%

The Regression Equation in Uncoded Units is given in Equation 4.

$$CORR\ RATE = 26.46 - 1.57\ ACID\ CONC - 8.65\ CHNP + 4.87\ MNO_2\ \ 0.833\ ACID\ CONC*ACID\ CONC. + 1.448\ CHNP*CHNP + 1.449\ MNO_2*MNO_2 + 0.841\ ACID\ CONC*CHNP - 0.846\ ACID\ CONC*MNO_2 - 2.315\ CHNP*MNO_2 \qquad (4)$$

Where CORR RATE = Corrosion rate in mm/yr
ACID CONC = Acid (H2SO4) concentration in mol/dm^3
CHNP = coconut husk nanoparticles in wt.%
MNO_2 = manganese oxide in wt. %

The main effect plot of H_2SO_4 concentration against corrosion rate, as imaged in Figure 5, shows that when the acid concentration is increased, the rate at which the specimen corrodes increases slightly. Although there is a weak or non-linear relationship between acid concentration and rate of corrosion, the line might have a very shallow slope.

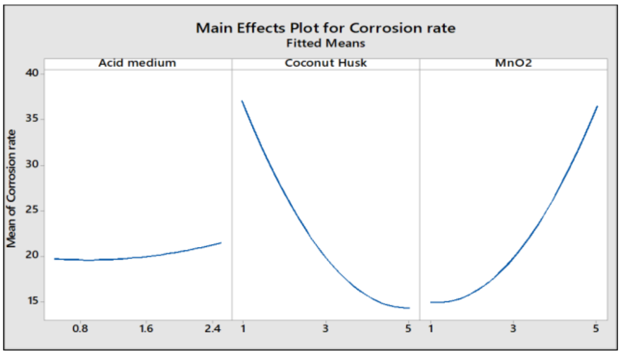

Figure 5: Main effect plot of Acidic medium (H_2SO_4), CHNPs and MnO_2 percentage composition against Corrosion rate.

A negative relationship between CHNP concentration and corrosion rate can be pictured as a downward-sloping line in the main effect plot. This indicates that increasing the CHNP content in the epoxy coating solution will likely cause a decrement in the corrosion rate. The positive relationship between corrosion rate and MnO_2 concentration is depicted by a positive slope in Figure 5. This implies that increasing the MnO_2 content in the epoxy coating solution will likely reduce its protective properties. This result is also corroborated by the contour plots of corrosion rate plotted in Figure 6.

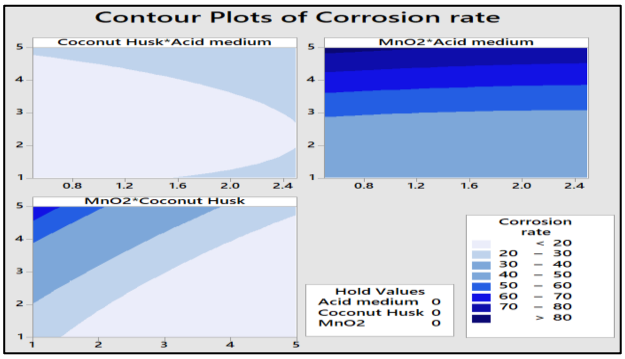

Figure 6: The contour plot of Acid concentration, MnO_2, CHNPs and corrosion rate

One can see from the contour plots that an increment in CHNP resulted in a reduced rate of corrosion, while an increment in MNO_2 resulted in an increased corrosion rate. Observing the MNO_2*Acid medium subsection of the contour plot, it can be resolved that the change in concentration of the acid medium did not affect the corrosion rate, but the CHNP*Acid medium subsection of the contour plot showed a slight effect on the corrosion rate as the concentration (in mol/dm^3) of the acid medium changes. It can be inferred that although CHNP provides better corrosion protection alone, its corrosion protection properties may be compromised by higher acid concentrations. This implies that better coating protection is guaranteed when MNO_2 is present, as acid concentration did not affect its corrosion protection. This validates the importance of MNO_2 in the coating composition, making it more useful in highly corrosive environments.
The optimisation plot generated is displayed in Figure 7. It can be seen that the optimal combination that will yield a minimum corrosion rate of 12.24mm/yr. at 0.9997 desirability is 0.5g/mol H_2SO_4, 4.43g CHNP and 2.05 MNO_2.

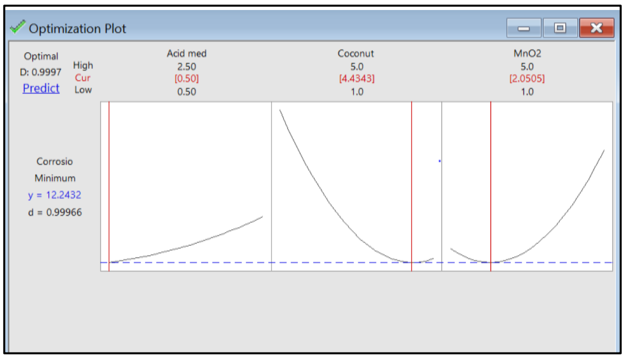

Figure 7: Optimization plot showing minimum corrosion rate

https://doi.org/10.4314/njt.v44i3.5

3.3 Coating Efficiency

The optimal combination, after validation, was utilised to get the efficiency of the developed coating. The PDP result for a blank (uncoated) and the optimal sample is tabulated in Table 8. It can be pictured that the corrosion rates for the blank and optimal samples are 219.9mm/yr. and 14.4mm/yr. respectively.

The corrosion efficiency of the coating was evaluated to be 93.7% using Equation 2.0.The surface morphology for the blank and optimal samples are given in Figure 8. It was captured with the aid of a Scanning Electron Microscope (SEM) equipment, Model (JOEL-JSM 7600F).

Table 8: PDP Result for Blank and Optimal Sample.

Sample	$E_{corr}(V)$	β_c (V/dec)	β_a(V/dec)	I_{corr} (A/cm^2)	Corrosion rate (mm/yr.)	$R_p(\Omega)$
Blank	-0.884	4.910	5.414	0.391287	219.96	0
Optimal	-0.896	5.604	6.534	0.016638	14.366	8

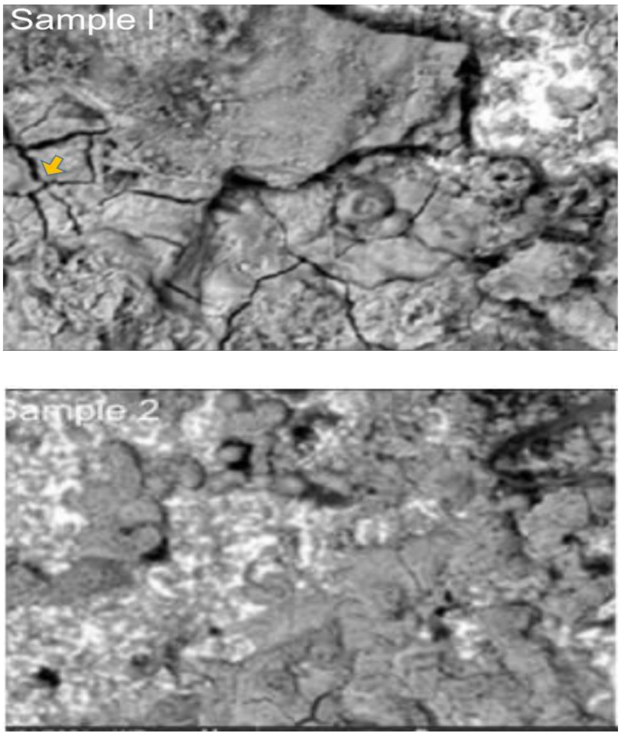

Figure 8: SEM images of corroded Blank (Sample 1) and Optimal coated (sample 2) specimen at 124μm of HFW

4.0 CONCLUSION AND RECOMMENDATION

4.1 Conclusion

The key findings derived from this research study can be summarized as follows.

- Synthesis of coconut shell nanoparticles through mechanical milling was achieved. The synthesized CHNPs were successfully used, in combination with MNO_2, as locally sourced low-cost natural nanoparticles for epoxy reinforcements in the production of a novel coating that can protect carbon steel from corrosion.
- Incorporation of CHNPs and MNO_2 in epoxy coating synergistically minimized corrosion rate and maximized charge transfer resistance. This synergy suggests a combined mechanism where CHNP's physical barrier restricts ionic ingress, while MNO_2 bolsters the steel's inherent passivity, offering a promising strategy for optimizing corrosion protection in harsh environments.
- Coating efficiency of 93.7% was obtained at 0.5 mol.dm^{-3} H_2SO_4, 4.45 wt.% CHNP, and 2.03 wt.% MNO_2

In summary, this work has shown the combined effect of manganese oxide and CHNP on the corrosion protection of steel pipes when incorporated into epoxy coating. The product is useful for the protection of the environment by reducing spills due to corrosion failures of pipelines and removing wastes from the environment. It also has economic benefits since the production can be done locally and could serve as a source of income.

4.2 Recommendation

The primary recommendations arising from this work, particularly for the CHNP/MNO_2 reinforced epoxy coating, include:

- Pilot tests in actual acidic environments relevant to specific industries should be carried out to validate the performance and efficacy of the developed coating.
- Wider tests should be carried out beyond the current range/scope of this research to explore the ability and compatibility with diverse media and specimens of the developed coating to protect other metals and materials from corrosion, to expand its application.

https://doi.org/10.4314/njt.v44i3.5

REFERENCES

[1] Ihamdane, R. Tiskar, M. Outemsaa, B. Zelmat, L. Dagdag, O. Berisha, A. Berdimurodov, E. Ebenso, E. and Chaouch, A "Essential Oil of Origanum vulgare as a Green Corrosion Inhibitor for Carbon Steel in Acidic Medium," *Arabian Journal for Science and Engineering,* 48, p. 7685–7701, 2023.

[2] Nguyen, T. Park, J. Kim, W. S. Nahm, S. H. and Beak, U. B "Effect of low partial hydrogen in a mixture with methane on the mechanical properties of X70 pipeline steel," *International Journal of Hydrogen Energy*, 45(3), pp. 2368-2381, 2020.

[3] Prasad, A. R. Kunyankandy, A. and Joseph, A. "Corrosion Inhibition in Oil and Gas Industry-Economic Considerations," in Corrosion Inhibition in Oil and Gas Industry, Saji, V. S. and Umoren, S. A. Eds., Wiley Online Library, 2020.

[4] Alamri, A. H. "Localized corrosion and mitigation approach of steel materials used in oil and gas pipelines – An overview," *Engineering Failure Analysis*, 116, 2020.

[5] WCO, "World Corrosion Organisation," 24 April 2024. [Online]. Available: https://corrosion.org/Events/Corrosion+Awareness+Day/2024_+April+24-p-2706.html. [Accessed 5 August 2025].

[6] Olugbode, M. "FG Decries Massive Effect of Corrosion on Nigeria's Economy," This Day, August 6 2023. [Online]. Available: https://www.thisdaylive.com/2023/10/25/fg-decries-massive-effect-of-corrosion-on-nigerias-economy/. [Accessed August 2025].

[7] Fotovvati, B. Namdari, N. and Dehghanghadikolaei, A. "On Coating Techniques for Surface Protection: A Review," *Journal of Manufacturing and Materials Processing*, 3(1), 2019.

[8] Sharun, V. Rajasekaran, M. Kumar, S. S. Tripathi, V. Sharma, R. Puthilibai, G. Sudhakar, M. and Negash, K. "Study on Developments in Protection Coating Techniques for Steel," *Advances in Materials Science and Engineering*, 2022, pp. 1-10, 2022.

[9] Tusher, M. Imam A. and Shuvo, M. "Future and Challenges of Coating Materials," in *Coating Materials. Materials Horizons: From Nature to Nanomaterials*, Verma, A. Sethi, S. and Ogata, S. Eds., Singapore, Springer, 2023.

[10] Desai, P. D. Pawar, C. B. Avhad, M. S. and More, A. P. "Corrosion inhibitors for carbon steel: A review," *Vietnam Journal of Chemistry*, 61(1), pp. 15-42, 2023.

[11] Wu, Y. Wu, Y. Sun, Y. Zhao, W. and Wang, L. "2D Nanomaterials Reinforced Organic Coatings for Marine Corrosion Protection: State of the Art, Challenges, and Future Prospectives," *Advanced Materials*, 36(37), pp. 1-31, 2024.

[12] Udoh, T. H. and Sunday, M. U. "Investigation of Corrosion Inhibition Potential of Selected Biological Inhibitors," *Nigerian Journal of Technology* (NIJOTECH), 41(2), pp. 263-269, 2022.

[13] Ajike, E. E. Lebe, A. N. N. E. C. Ogwo, K. D. and Ahamfula, C. Y. "Inhibitive Properties of Garcinia Kola (GK) in Alkaline Medium of Aluminium Alloy (AA4007)," *Nigerian Journal of Technology* (NIJOTECH), 43(2), pp. 272-278, 2024.

[14] Sun, H. Li, L. and Li, W. "Application of organosilanes in titanium-containing organic–inorganic hybrid coatings," *Journal of Materials Science*, 57(29), pp. 13845–13870, 2022.

[15] Ragheb, D. M. Abdel-Gaber, A. M. Mahgoub, F. M. and Mohamed, M. E. "Eco-friendly method for construction of superhydrophobic graphene-based coating on copper substrate and its corrosion resistance performance," *Scientific Reports*, 12, 2022.

[16] Yue, P. Zhang, M. Zhao, T. Liu, P. Peng, F. and Yang, L. "Eco-friendly epoxidized Eucommia ulmoides gum based composite coating with enhanced super-hydrophobicity and corrosion resistance properties," *Industrial Crops and Products*, 214, 2024.

[17] Ouarga, A. Lebaz, N. Tarhini, M. Noukrati, H. Barroug, A. Elaissari A. and Youcef, H. B. "Towards smart self-healing coatings: Advances in micro/nano-encapsulation processes as carriers for anti-corrosion coatings development," *Journal of Molecular Liquids*, 354, 2022.

[18] Aramayo, M. A. F. and Aoki, I. V. "Self-healing capability of epoxy coating using dual-component microcapsules under immersion," *Journal of Iron and Steel Research International*, 32(5), 2025.

[19] Thomas, D. Philip, R. R, E. Sindhu, R. Ulaeto, S. B. Pugazhendhi, A. and Awasthi, M. K.

https://doi.org/10.4314/njt.v44i3.5

"Developments in smart organic coatings for anticorrosion applications: a review," *Biomass Conversion and Biorefinery*, 12, pp. 4683–4699, 2022.

[20] Kumari, S. and Saini, A. D. V. "Metal oxide based epoxy coatings for corrosion protection of steel," *Materials Today: Proceedings*, vol. 43, pp. 3105-3109, 2021.

[21] Eskandari, M. Shanaghi, A. Kamani, M. and Niari, M. A. "Effect of nano-metal oxides (ZnO, Al2O3, CuO, and TiO2) on the corrosion behaviour of a nano-metal oxide/epoxy coating applied on the copper substrate in the acidic environment," *Applied Nanoscience*, 11(5), pp. 1605–1615, 2021.

[22] Muresan, L. M. "Nanocomposite Coatings for Anti-Corrosion Properties of Metallic Substrates," *Materials*, vol. 16, no. 14, 2023.

[23] Ashibudike, O. E. Iweriolor S. and Oreko, B. U. "Electrochemical Corrosion Inhibition of Cobalt-Graphene Nano-Composite on Mild Steel in Acidic Corrosion Environment," *Nigerian Journal of Technology* (NIJOTECH), 43(2), pp. 261-271, 2024.

[24] Azani, N. F. S. M. Zahari, H. M. M. A Sophie, P. Brosse, N. and Hazwan, M. H. "Preparation and characterizations of oil palm fronds cellulose nanocrystal (OPF-CNC) as reinforcing filler in epoxy-Zn rich coating for mild steel corrosion protection," *International Journal of Biological Macromolecules*, 353, pp. 385-398

[25] Oisakede, M. "Evaluation of the Thermal properties of Epoxy-Agro waste (Egg shell and Palm kernel shell) Nanoparticle coating for Mild Steel.," *Black Sea Journal of Engineering and Science*, 4(4), pp. 179-182, 2021.

[26] Vaithilingam, S. ThangavelRavivarman, R. and Muthukaruppan, A "Development of cashew nut shell carbon reinforced thiourea based biophenolic benzoxazine-epoxy composites: High performance biobased coating materials," *Polymer Composites*, 41(5), pp. 1950-1961, 2020.

[27] Azadi, M. Mehrabadi, M. and Hafazeh, A. "The corrosion inhibition efficiency of carbon steel in HCl solution utilizing pistachio soft hull extract: Experimental measurements, DFT and MD simulations," *Results in Engineering*, 26, pp. 1-13, 2025.

[28] Ossila, "Ossila BV," 15 February 2025. [Online]. Available: https://www.ossila.com/products/manganese-iv-oxide-powder.

[29] Rudawska, A. Gola, A. Pizo ́n, J. Capała, P. and Wójcik, Ł. "Effectiveness of Bonding Steel Elements with Polyester-Coated Paint," *Applied Sciences*, 13(18), pp. 1-16, 2023.

https://doi.org/10.4314/njt.v44i3.5